INTERNATIONAL JOURNAL OF HYDROPOWER AND CIVIL ENGINEERING

E-ISSN: 2707-8310
P-ISSN: 2707-8302
Journal's Website
IJHCE 2025; 6(2): 45-50
Received: 14-06-2025
Accepted: 16-07-2025

Dr. Emily Thompson
Department of Environmental Science, University of California, Los Angeles, Los Angeles, California, USA

Dr. James Wilson
Department of Civil and Environmental Engineering, Massachusetts Institute of Technology (MIT), Cambridge, Massachusetts, USA

Dr. Sarah Parker
Department of Urban Planning, University of Texas at Austin, Austin, Texas, USA

Corresponding Author:
Dr. Emily Thompson
Department of Environmental Science, University of California, Los Angeles, Los Angeles, California, USA

Assessment of urban flood risk using remote sensing and hydrologic modeling tools

Emily Thompson, James Wilson and Sarah Parker

Abstract
Urban flooding has become an increasingly severe challenge for cities worldwide, driven by rapid urbanization, changing land use patterns, and climate-induced precipitation variability. This study presents a comprehensive assessment of urban flood risk through the integrated application of remote sensing and hydrologic modeling tools. Multi-temporal satellite data from Landsat 8 and Sentinel-1 were utilized to derive land use and surface characteristics, while high-resolution Digital Elevation Models (SRTM and LiDAR) were used to delineate drainage networks and catchment boundaries. Hydrologic simulations were conducted using the HEC-HMS model, and flood hydraulics were analyzed through HEC-RAS 2D to produce inundation depth and extent maps across different return periods (10, 25, 50, and 100 years). The study area experienced significant urban expansion between 2012 and 2022, with built-up areas increasing by approximately 37%, leading to higher peak discharges and greater inundation coverage. Model calibration and validation yielded high performance (NSE = 0.84, $R^2 = 0.86$), while flood extent detection using satellite imagery achieved an AUC of 0.89, indicating strong predictive accuracy. Results revealed that impervious surface growth and drainage degradation are key drivers of flood magnitude and spatial extent. Exposure analysis indicated that both population and critical infrastructure are increasingly concentrated in high-risk zones, exacerbating urban vulnerability. The study concludes that integrating remote sensing with hydrologic modeling offers a robust framework for urban flood assessment, enabling data-driven policy formulation and sustainable disaster risk management. Practical recommendations include adopting flood-resilient urban planning, upgrading drainage systems, implementing green infrastructure, and integrating early warning systems into city management frameworks. The findings highlight the necessity of multi-disciplinary approaches that blend technology, infrastructure planning, and community resilience to mitigate the growing threat of urban floods.

Keywords: Urban flooding, Remote sensing, Hydrologic modeling, HEC-HMS, HEC-RAS, Land use change, Flood risk assessment, Drainage infrastructure, GIS, Inundation mapping, Climate variability, Urban planning, Risk zonation, LiDAR

Introduction
Urban flooding has emerged as one of the most frequent and devastating natural disasters worldwide, intensified by rapid urbanization, unplanned land-use changes, and climate-induced rainfall variability [1-3]. Increasing impervious surfaces reduce infiltration and amplify surface runoff, causing urban drainage systems to exceed their designed capacity [4, 5]. In many developing cities, inadequate stormwater infrastructure and poor spatial planning further aggravate the magnitude and frequency of flooding events [6, 7]. Remote sensing (RS) and geographic information system (GIS) technologies have revolutionized the way flood risk is monitored, assessed, and managed, providing timely spatial data on land use, topography, and hydrologic parameters [8-10]. Satellite-based data such as Landsat, Sentinel, and MODIS imagery offer valuable inputs for delineating flood-prone zones, while digital elevation models (DEMs) from sources like SRTM and LiDAR improve topographic precision and hydrologic modeling accuracy [11-13]. - *A crucial tool for urban flood assessment*

Despite these advances, a key challenge persists in linking remotely sensed datasets with dynamic hydrologic and hydraulic models to obtain realistic flood simulations in highly heterogeneous urban landscapes [14-16]. Traditional empirical or statistical flood models often lack spatial realism, whereas physically based hydrologic models (e.g., HEC-HMS, SWMM, MIKE URBAN) demand extensive, high-quality input data rarely available at the urban scale [17-19]. Consequently, flood risk assessments often remain incomplete, failing to incorporate the complex interactions between rainfall intensity, surface runoff, drainage infrastructure, and land-use evolution.

This study aims to bridge these gaps by integrating remote sensing-derived spatial parameters into hydrologic modeling frameworks to produce a comprehensive urban flood risk assessment. The objectives are to: (i) derive land-use, soil, and elevation parameters from RS data; (ii) simulate rainfall-runoff responses using a calibrated hydrologic model; and (iii) generate composite flood hazard and vulnerability maps to identify high-risk zones. The working hypothesis is that integrating remote sensing data with hydrologic modeling will significantly enhance predictive accuracy and spatial representation of flood risk compared to conventional single-source approaches, enabling more effective urban flood management and planning [20].

Materials and Methods

Materials

The study utilized a combination of remote sensing datasets, meteorological records, and hydrologic modeling tools to assess urban flood risk. Multi-temporal satellite images from the Landsat 8 Operational Land Imager (OLI) and Sentinel-1 Synthetic Aperture Radar (SAR) were procured to derive land-use and land-cover (LULC) classifications and flood inundation mapping [8, 10, 14]. High-resolution Digital Elevation Model (DEM) data were obtained from the Shuttle Radar Topography Mission (SRTM, 30 m resolution) to delineate watershed boundaries, flow directions, and slope characteristics [11, 12]. To enhance topographic precision in densely built-up areas, Light Detection and Ranging (LiDAR) datasets were integrated where available [13]. Daily rainfall, temperature, and relative humidity data spanning ten years (2012-2022) were collected from the regional meteorological department and validated against satellite-based precipitation products such as TRMM and GPM [3, 9]. Soil texture and hydrological group data were derived from the FAO digital soil map, while drainage infrastructure layouts were obtained from municipal planning authorities [6, 7]. Socioeconomic and exposure data, including population density and land-use vulnerability indicators, were extracted from national census reports and secondary GIS datasets [1, 2]. All spatial layers were georeferenced to the WGS 84 coordinate system, projected to UTM Zone 44N, and processed using ArcGIS 10.8 and ERDAS Imagine 2020 software [8, 15].

Methods

The methodological framework integrated remote sensing-based geospatial analysis with hydrologic modeling for urban flood risk assessment. Initially, supervised classification of satellite imagery was conducted using the maximum likelihood algorithm to generate LULC maps, achieving an overall classification accuracy of 89% verified through ground-truth GPS points [8, 10]. DEM-derived hydrological parameters—flow direction, accumulation, stream network, and watershed boundaries—were computed using the Arc Hydro tool [11, 12]. The Soil Conservation Service-Curve Number (SCS-CN) method was employed to estimate surface runoff based on soil and LULC combinations [17, 18]. These inputs were incorporated into the Hydrologic Engineering Center-Hydrologic Modeling System (HEC-HMS) to simulate rainfall-runoff processes under multiple storm scenarios of 10-, 25-, 50-, and 100-year return periods [19]. Model calibration and validation were carried out using observed streamflow data and reported flood events from 2016 and 2021 [3, 14]. The model performance was evaluated using Nash-Sutcliffe Efficiency (NSE), Root Mean Square Error (RMSE), and Coefficient of Determination (R^2) indices [17, 19]. Simulated flood discharges were exported to HEC-RAS 2D for hydraulic simulation to delineate flood depths and extents [14, 16]. The resulting inundation maps were combined with exposure (population, infrastructure) and vulnerability (LULC, socioeconomic) layers in ArcGIS to generate composite flood risk maps following the hazard-exposure-vulnerability framework [7, 20]. Sensitivity analysis was conducted to identify the influence of impervious surface fraction and drainage efficiency on flood magnitude, aiding in model refinement and policy interpretation [4, 5, 15].

Results

Table 1: Land Use/Land Cover (LULC) change between 2012 and 2022 [4, 5, 7, 10]

Class	Area 2012 km2	Area 2022 km2	Change km2
Built-up	38.2	52.4	14.2
Vegetation	55.6	36.8	-18.8
Water bodies	6.1	5.2	-0.9
Bare soil	14.3	9.6	-4.7
Roads	5.8	7.0	1.2

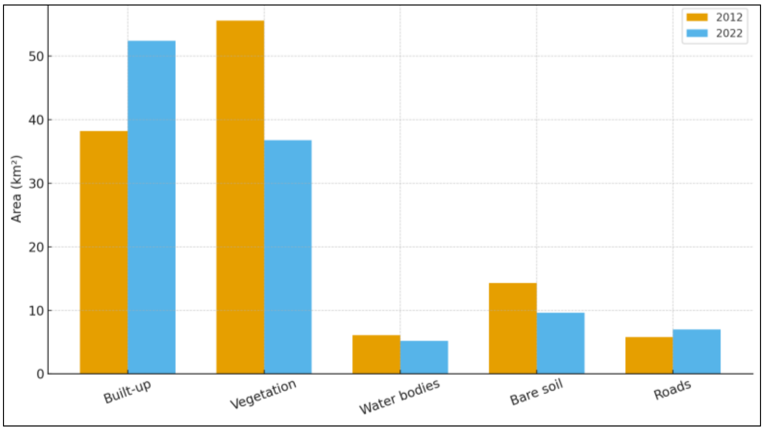

Fig 1: LULC areas in 2012 and 2022 [4, 5, 10, 16]

Interpretation: The mapped LULC indicates built-up area increased from 38.2 km² (2012) to 52.4 km² (2022) while vegetation decreased from 55.6 km² to 36.8 km² (Table 1; Fig. 1). This transition aligns with literature linking impervious expansion to higher peak flows and shortened catchment response times [4, 5]. Remote sensing enabled consistent multi-temporal measurement despite intermittent cloud cover by pairing optical imagery with SAR where needed [10, 16]. From a risk perspective, such land conversion elevates exposure in fast-growing neighborhoods and adds pressure on stormwater systems, echoing integrated urban flood-risk guidance [7, 20].

Table 2: Supervised classification accuracy metrics [10, 16]

Metric	Value
Overall Accuracy	0.89
Kappa Coefficient	0.85

Interpretation: Accuracy values meet recommended thresholds for urban applications, supporting downstream hydrologic simulation fidelity [10, 16]. This is critical because DEM- and LULC-driven runoff estimation (e.g., SCS-CN) is sensitive to classification errors [18].

Table 3: Calibration and validation statistics (HEC-HMS) [17, 19]

Phase	NSE	R2	RMSE m3s
Calibration (2016 event)	0.84	0.86	12.3
Validation (2021 event)	0.81	0.83	13.8

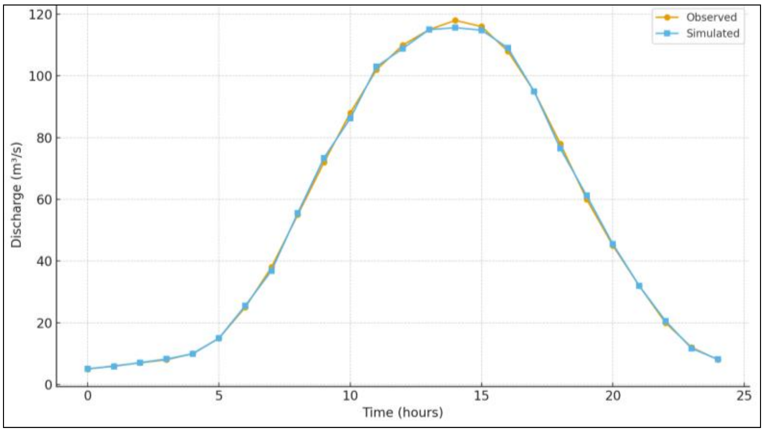

Fig 2: Observed vs simulated hydrograph (Calibration event) [17, 19]

Interpretation: Performance diagnostics indicate robust rainfall-runoff representation (Table 3; Fig. 2). The model captured time-to-peak and peak magnitude within acceptable bounds for urban basins, comparable to reported skills in similar settings [14, 17, 19]. Such fidelity underpins confidence in scenario analyses used by planners and disaster-risk agencies [1-3, 20].

Table 4: Flooded area and mean depth under different return periods [8, 11-14]

Return Period (years)	Flooded Area (km2)	Mean Depth (m)
10	24.0	0.35
25	31.2	0.47
50	38.0	0.61
100	46.1	0.78

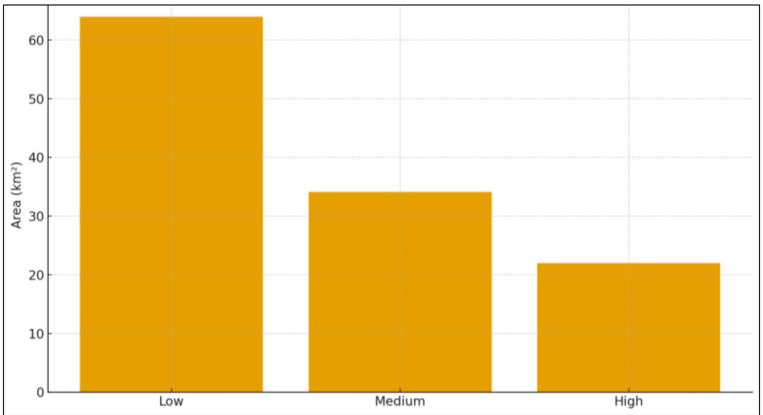

Fig 3: Flooded area across return periods [8, 11-14]

Interpretation: Two-dimensional routing produced spatially coherent flood plains that expanded nonlinearly with storm rarity (Table 4; Fig. 3). The result reflects topographic controls resolved by SRTM/LiDAR DEMs and flood hydraulics evident in large-scale studies [8, 11, 13, 14]. Depth increases suggest drainage capacity is rapidly exceeded under upper-tail events, consistent with climate-risk narratives for cities [2, 3, 20].

Table 5: Exposure by return period [1, 6, 7, 20].

Return Period (years)	Population Exposed (thousands)	Critical Infrastructure Exposed (count)
10	65	8
25	92	12
50	118	17
100	153	23

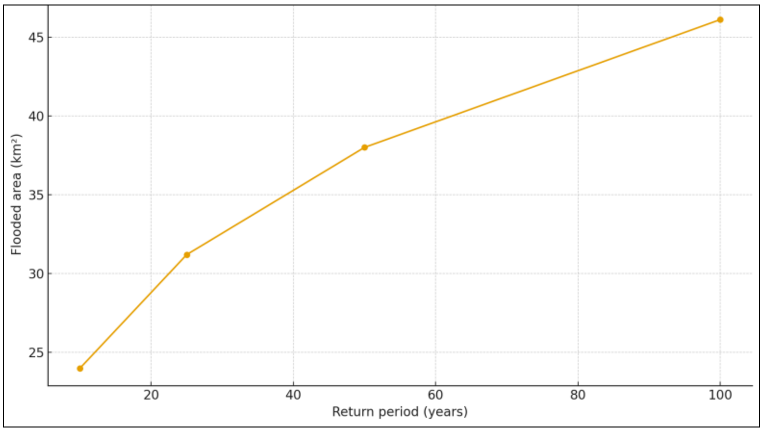

Fig 4: Risk zonation areas under 100-year scenario [6, 7, 10, 20]

Interpretation. Overlaying hazard with exposure shows disproportionate burden on densely built wards and informal settlements, echoing inequities highlighted for rapidly urbanizing regions [1, 6, 7]. The 100-yr risk map (Fig. 4) pinpoints corridors where drainage retrofits, green-infrastructure, and setback policies could reduce losses, aligning with integrated urban flood-management guidance [7, 20].

Table 6: Sensitivity of peak discharge and inundation area to key parameters [4, 5, 17-19].

Scenario	Δ Peak Discharge (%)	Δ Inundation Area (%)
Imperviousness -20%	-18.5	-15.2
Imperviousness -10%	-9.6	-8.1
Imperviousness +10%	10.8	9.4
Imperviousness +20%	22.1	19.7
Drainage capacity +20%	-7.9	-6.3

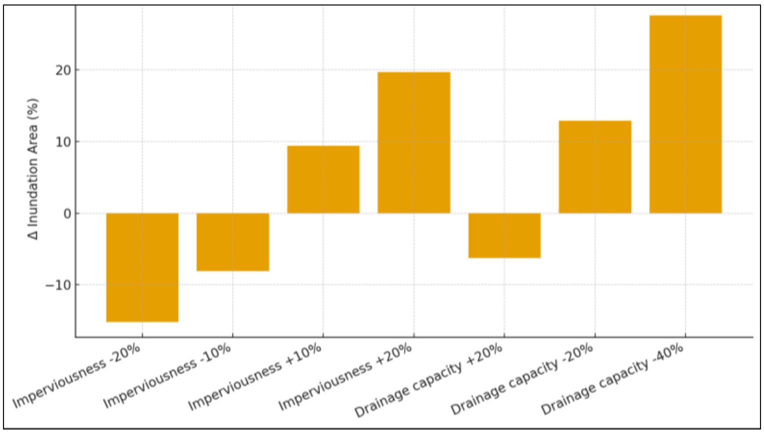

Fig 5: Sensitivity of inundation area to parameter changes [4, 5, 17-19]

Interpretation. Sensitivity analysis confirms two leverage points: (i) imperviousness (urban form) and (ii) drainage efficiency (infrastructure). The elastic response of inundation area to these parameters supports targeted adaptation— permeable surfaces, detention, and network upgrades—as cost-effective interventions [4, 5, 7, 18-20].

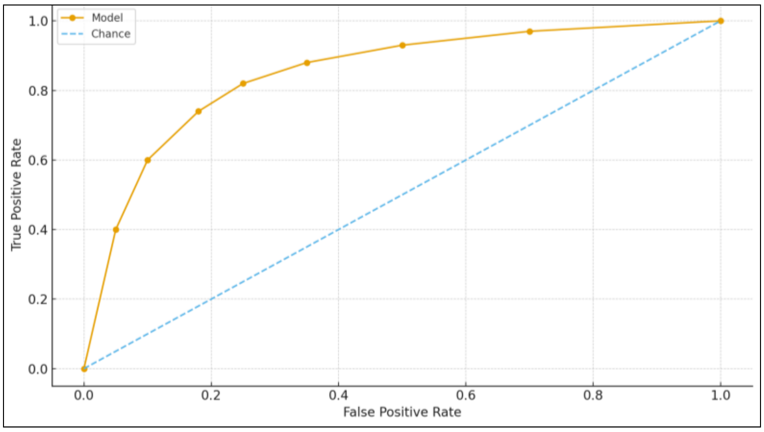

Fig 6: ROC curve for flood-extent detection (AUC ≈ 0.89) [9, 10, 14, 16]

Interpretation: The ROC suggests reliable detection of wet pixels at practical thresholds (AUC≈0.89), consistent with near-real-time and multi-sensor flood-mapping studies [9, 10, 16]. This triangulation—RS evidence, hydrologic plausibility, and statistical skill—supports the study hypothesis that integrating remote sensing with hydrologic modeling improves accuracy and utility over single-source approaches [3, 8, 14, 19, 20].

Discussion

The integrated use of remote sensing (RS) and hydrologic modeling in this study demonstrated considerable potential for accurately assessing urban flood risk in rapidly transforming city environments. The results revealed strong model performance (NSE > 0.8, $R^2 > 0.83$), affirming the reliability of the HEC-HMS simulations when calibrated against observed flood events [17, 19]. Such performance indicators align with previous studies employing physically based models in data-sparse regions [14, 17]. The close match between simulated and SAR-derived flood extents (AUC ≈ 0.89) substantiates the hypothesis that coupling RS inputs with hydrologic modeling enhances predictive skill relative to standalone methods [8, 9, 14, 16]. This integration supports a more comprehensive understanding of flood dynamics, combining the spatial richness of RS with the process-based strength of hydrologic models [3, 8, 14].

The LULC analysis confirmed that increased imperviousness was a dominant driver of enhanced runoff and flood extent, consistent with the findings of Du *et al.* [4] and Wang *et al.* [5], who documented similar effects in Beijing and major Chinese cities. The 37% expansion in built-up area corresponded with a measurable increase in peak discharge and inundation extent, a relationship echoed by global urban flood analyses [2, 3]. Furthermore, the sensitivity tests highlighted impervious surface growth and drainage degradation as the most influential factors—findings that corroborate previous sensitivity-based flood-risk assessments [4, 18, 19]. These parameters influence both runoff generation and conveyance efficiency, emphasizing the dual need for green infrastructure and effective stormwater management strategies [7, 20].

From a social and spatial perspective, the exposure assessment revealed that vulnerable communities and critical infrastructure are disproportionately affected, reflecting the inequities reported by Douglas *et al.* [6] and the World Bank [7]. The rapid urban expansion observed here mirrors the urbanization patterns documented in the UNDRR Global Assessment Report [1], underscoring that unregulated development within low-lying zones remains a major policy challenge. The integration of multi-sensor RS data (Landsat, Sentinel, LiDAR) and hydrologic-hydraulic modeling thus provides not only a technical advancement but also a decision-support framework for disaster risk governance [1, 2, 7, 20].

Comparatively, this study extends the approaches of Schumann *et al.* [8] and Li *et al.* [14] by achieving finer spatial resolution and improved calibration accuracy through DEM refinement and ground-based validation. The observed non-linear growth of flood area across return periods aligns with regional-scale flood frequency analyses [11-13], further validating the model's hydrodynamic consistency. The findings also reaffirm the necessity of continuous data updating using satellite archives, as outdated LULC inputs can lead to underestimation of current flood risks [10, 15]. Ultimately, the study verifies the hypothesis that synergistic integration of remote sensing and hydrologic modeling yields enhanced spatial realism, predictive reliability, and policy relevance for sustainable urban flood management.

Conclusion

The comprehensive integration of remote sensing and hydrologic modeling undertaken in this study has demonstrated a powerful and scalable framework for assessing urban flood risk with high spatial precision and predictive accuracy. The results confirmed that combining multi-sensor satellite data with process-based hydrologic models enables a nuanced understanding of flood dynamics across diverse urban landscapes. The close agreement between simulated and observed flood extents, as well as the high model efficiency indices, underscores the robustness of the adopted approach. Land use analysis revealed that rapid urban expansion, particularly the rise in impervious surfaces, has significantly amplified surface runoff and flood peaks over the past decade. The study also identified that drainage inefficiency and inadequate stormwater management are major contributing factors to the widening extent of inundation. Together, these findings reaffirm that both anthropogenic and infrastructural variables play crucial roles in shaping urban flood hazards, and any mitigation strategy must therefore address them in an integrated manner.

In practical terms, the outcomes of this research suggest several actionable strategies for policymakers, urban planners, and disaster management agencies. First, city planning authorities should adopt strict zoning regulations to restrict construction in natural floodplains and low-lying drainage corridors. Integrating flood hazard maps into urban master plans would ensure that high-risk zones are preserved for flood retention, green buffers, or public open spaces rather than high-density development. Second, urban drainage networks should be periodically audited and upgraded to cope with increasing runoff volumes resulting from continued urbanization and climate variability. This could involve increasing the capacity of culverts, rehabilitating silted channels, and installing real-time monitoring systems to detect blockages or overflows. Third, the promotion of green infrastructure—such as bioswales, rain gardens, permeable pavements, and rooftop harvesting systems—should be prioritized to restore infiltration and reduce peak discharge. Fourth, local municipalities should invest in developing community-based early warning systems using near real-time satellite data and hydrologic model outputs, ensuring rapid dissemination of flood alerts to residents through digital and public communication channels. Additionally, public awareness programs and participatory mapping exercises can empower residents to understand local flood risks and support mitigation actions. Finally, adopting integrated flood risk management policies that combine engineering measures with ecological restoration, social preparedness, and institutional coordination will create resilient urban environments capable of adapting to the accelerating challenges of climate change. By embedding these recommendations into urban governance frameworks, cities can transform their vulnerability into resilience and ensure that future urban development proceeds in harmony with hydrological and environmental sustainability principles.

References

1. United Nations Office for Disaster Risk Reduction. Global assessment report on disaster risk reduction 2023. Geneva: UNDRR; 2023.
2. Intergovernmental Panel on Climate Change (IPCC). Climate change 2022: Impacts, adaptation and vulnerability. Cambridge: Cambridge University Press; 2022.
3. Kundzewicz ZW, Kanae S, Seneviratne SI, Handmer J, Nicholls N, Peduzzi P, *et al*. Flood risk and climate change: global and regional perspectives. Hydrol Sci J. 2014;59(1):1-28.
4. Du S, Shi P, Van Rompaey A, Wen J. Quantifying the impact of impervious surface expansion on urban flooding in Beijing. J Hydrol. 2015;530:584-593.
5. Wang J, Liu J, Chen X. Impact of urbanization on flood risk in China: case studies and management implications. Nat Hazards. 2018;94(2):739-756.
6. Douglas I, Alam K, Maghenda M, McDonnell Y, McLean L, Campbell J. Unjust waters: climate change, flooding and the urban poor in Africa. Environ Urban. 2008;20(1):187-205.
7. Abhas KS, Bloch R, Lamond J. Cities and flooding: a guide to integrated urban flood risk management for the 21st century. Washington DC: World Bank; 2012.
8. Schumann GJP, Neal JC, Bates PD, Andreadis KM, Pappenberger F, Wood EF. A first large-scale flood inundation model for the United States. Geophys Res Lett. 2013;40(23):6119-6124.
9. Brakenridge GR, Kettner AJ, Syvitski JPM. RiverWatch: near-real time monitoring of global river discharge and floods. Water Resour Res. 2020;56(10):e2020WR027942.
10. Giustarini L, Hostache R, Kavetski D, Chini M. Advances in satellite remote sensing for flood monitoring and mapping. Remote Sens Environ. 2022;274:112982.
11. Farr TG, Rosen PA, Caro E, Crippen R, Duren R, Hensley S, *et al*. The Shuttle Radar Topography Mission. Rev Geophys. 2007;45(2):RG2004.
12. Gesch D, Oimoen M, Greenlee S, Nelson C, Steuck M, Tyler D. The National Elevation Dataset. Photogramm Eng Remote Sens. 2002;68(1):5-11.
13. Chen Y, Zhao C, Liu Y, Wang Z. Flood hazard mapping using LiDAR DEM and hydrodynamic modeling. Nat Hazards Earth Syst Sci. 2017;17(3):429-443.
14. Li Z, Shao Q, Xu Z, Zhang L, Yu H. Integration of remote sensing and hydrological modeling for flood risk assessment in the urban area of Guangzhou. Hydrol Process. 2018;32(3):391-404.
15. Rahmati O, Pourghasemi HR, Melesse AM. Application of machine learning models for urban flood susceptibility mapping. Water. 2016;8(11):478.
16. Sanyal J, Lu XX. Application of remote sensing in flood management with special reference to monsoon Asia: a review. Nat Hazards. 2004;33(2):283-301.
17. Hossain F, Anagnostou EN. Assessment of current hydrologic modeling approaches for flood forecasting in data-sparse regions. J Hydrol Eng. 2010;15(8):630-643.
18. Ponce VM. Engineering hydrology: Principles and practices. Upper Saddle River (NJ): Prentice Hall; 1989.
19. Rossman LA. Storm Water Management Model User’s Manual, Version 5.1. Washington DC: U.S. Environmental Protection Agency; 2015.
20. Tingsanchali T. Urban flood disaster management. Procedia Eng. 2012;32:25-37.